

# Stability analysis of a human-influenced landslide in eastern Belgium

Thomas Preuth<sup>a,\*</sup>, Thomas Glade<sup>b</sup>, Alain Demoulin<sup>c</sup>

<sup>a</sup> WSL Swiss Federal Institute for Snow and Avalanche Research SLF, Flüelastasse 11, CH-7260 Davos, Switzerland

<sup>b</sup> Institute for Geography and Regional Sciences, University of Vienna, Universitätsstrasse 7, 1010 Vienna, Austria

<sup>c</sup> Department of Physical Geography and Quaternary, University of Liège, Sart Tilman, B11, 4000 Liège, Belgium

## ARTICLE INFO

### Article history:

Accepted 7 August 2009

Available online 24 September 2009

### Keywords:

Complex landslide

Soil chemistry

Human impact

Belgium

## ABSTRACT

The area of the Pays de Herve in eastern Belgium is strongly affected by recent landslide activity. Dormant landslides are widespread in the region and some of these dormant landslides have been reactivated by human activity such as highway construction, suburban development, or building of industrial sewage pipes. The investigated landslide was reactivated by heavy rainfall events in the late 1990s. During this reactivation an existing industrial sewage pipe was damaged and the chemically loaded waste water drained into the landslide mass. The current landslide movement is assumed to be heavily influenced by the additional water supply as well as by the chemical activity of univalent ions in the clay fraction leading to a decreased shear resistance. Consequently, the movement-triggering rainfall thresholds are reduced and result in a decreased overall slope stability.

This study describes a general methodology of field investigation, data collection and laboratory testing for an exploratory study. Influences of chemical properties of soil and soil water and their effects on landslide stability are analysed, discussed and related to findings of other studies. Although no clear empirical evidence for a dependency between slope stability and ionic loaded soil water was found in this study, we suggest the existence for such a relationship. We conclude that this particular landslide would not have moved based on current environmental conditions. The leaking waste water might favour current landslide movement.

© 2009 Elsevier B.V. All rights reserved.

## 1. Introduction

The influence of human activity on geosystems is not a new topic in geomorphology and is addressed in recent discussions (Barnard et al., 2001; Glade, 2003; Remondo et al., 2005; Goudie, 2006). Some emerging questions are: Did human actions impact on geomorphic systems? How are magnitude and frequency of processes influenced and by which factors? Examples of human interactions favouring landslide failures are the construction of water supply dams, which change the water balance in the environment (Hendron and Patton, 1987; Gillon et al., 1991), sealing of ground by constructing roads and other infrastructure, which increases pore pressures due to reduced drainage capacities, and cutting slopes for suburban development (Hancox, 2002; Glade et al., 2005).

Geomorphic systems, and specifically slope systems, are determined by the current development stage of a specific landscape and the influences of the recent environment (Anderson and Richards, 1987). Such conditions provide internal and external stability factors including slope angle, slope length, climate, geotechnical material properties (Crozier, 1989). Slope systems naturally evolve toward a condition of stability with time thus increasing their resistance to

external forces. But if an external force exceeds a critical threshold and occurs with sufficiently high magnitude and/or frequency, even previously stable systems might fail. One of these external factors can be human impact.

The influence of geochemical changes of soil properties for slope stability is only partially covered in literature (Kronberg and Nesbitt, 1981; Veder and Hilbert, 1981; Czurda and Xiang, 1993; Gudehus and Külzer, 2002). Czurda and Xiang (1993) have intensively investigated the ionic influences on clay layer stability on a landslide in the Austrian Alps. Another example is the Abbotsford Landslide in New Zealand in 1979. The predispositional factors for this landslide included sensitive geological settings and the presence of a leaking water main located upslope the landslide mass. Hancox (2002) mentions the likelihood of a high dependency between a leaking water supply pipe and slope stability, however, there was no empirical evidence.

The present study focuses on a particular linkage between human actions and slope stability. Humanly induced landslides are quite common in landslide investigation (e.g. Barnard et al., 2001; Hancox, 2002; Runqui and Lungsang, 2003). A slope system in the Pays de Herve in eastern Belgium is described and analysed. In the Pays de Herve are numerous relict landslides which appear at least dormant or even stable in undisturbed conditions. However, numerous landslides have been reactivated by human interference, in particular by infrastructural work at railways and highways.

\* Corresponding author.

E-mail address: [preuth@slf.ch](mailto:preuth@slf.ch) (T. Preuth).

The aim of this study is manifold. The traditional Factor of Safety ( $F$ ) analysis is applied to calculate slope stability for current conditions. The possible human influence on a landslide is explored. The question whether chemical contamination might affect slope stability is discussed. The hypotheses for this study include the following:

- The current localized instability at Manaihan is the result of a human impact.
- The installation of the sewage pipe in the late 1960s led to an increased sensitivity of the affected slope.
- The water leaking into the sensitive layers of the slope has a considerable influence on the general slope stability.
- The landslide is always near the critical initiation threshold.

To provide a background for this study, general principles of soil mechanics relating to soil stability are reviewed. The introduction of the research area is followed by a description of methods and techniques employed. The next section deals with the results of the field measurements. Finally the results are discussed with respect to the introduced hypotheses. In conclusion, some perspectives are given on future research on physicochemical influences on slope stability.

## 2. Background

A brief landslide description, the type of movement and the geometry, the basics of slope stability modelling and the main factors potentially influencing slope stability are based on the work of Nash (1987), Craig (1992), Hartge and Horn (1991) and Lang et al. (2003). Cruden and Varnes (1996) describe the general features of a similar landslide (Fig. 1). General landslide geometry is described in Nash (1987) and Lang et al. (2003). Based on Crozier (1989), Glade et al. (2005) attribute failure conditions to preparing, triggering and controlling factors. While preparing factors increase the sensitivity of a slope to external factors without initiating a landslide, triggering factors initiate the movement. Controlling factors (e.g. slope angle, surface roughness, slope cover, slope material) dominate the movement pattern and in particular the velocity of the landslide.

The basic slope failure condition is defined by the Mohr–Coulomb equation:

$$\tau_f = c + (\sigma - u) \tan(\varphi) \quad (1)$$

where  $\tau_f$  is the shear stress at failure (referred to as shear strength),  $c$  is the cohesion,  $\sigma$  is the normal stress,  $u$  is the pore water pressure and  $\varphi$  is the internal friction angle. Failure is considered to take place when  $\tau$  (shear stress) is larger than  $\tau_f$ . Because the shear strength is in particular related to solid soil particles (Craig, 1992; Lang et al., 2003), it is a function of the effective forces, and so Eq. (1) changes to

$$\tau_f = c' + \sigma' \tan(\varphi') \quad (2)$$

This failure condition of Mohr–Coulomb is still the easiest and most used criterion to evaluate slope stability. The crucial factor in all stability studies is the Factor of Safety ( $F$ ), which describes the relationship between resisting and driving forces:

$$F = \frac{\tau_f}{\tau} = \frac{c' + \sigma' \tan(\varphi')}{\tau} \quad (3)$$

The type of model to determine  $F$  depends on the landslide type. Most models for translational and rotational slides assume distinct rupture plane(s), either parallel to the slope surface or circular in form. Other models assume non-linear forces within the slope (Nash, 1987) or instability progression along a shear plane (Petley et al., 2005). The crucial issue is that models simplify the highly complex reality of slope failure while retaining the main parameters (Lang et al., 2003). In general, the geometry of the slope is simplified to a profile shape, and it is assumed that failure occurs along either a planar or a circular shear plane (Nash, 1987; Lang et al., 2003). Commonly, the sliding mass is considered to be a sliding block.

Soil mechanical properties and consequent slope stability are also dependent on physicochemical factors (Zaruba and Mencl, 1969; Veder and Hilbert, 1981; Czurda and Xiang, 1993; Schachtschabel et al., 2003). Clay minerals are products of intense chemical weathering of rock and are crystallized OH-containing aluminosilicates with a flat structure. The mean length of clay minerals is about 2  $\mu\text{m}$  and the thickness is below 50 nm. These characteristics force clay soils to swell and to shrink and to show plastic material behaviour when in contact with water. Most important, clay minerals are able to adsorb or desorb ions. Depending on the ions between the ligands of the clay mineral, these build a tetrahedral or an octahedral form. Some of these aggregated ligands influence the forces between the clay minerals (Fig. 2a). The ions can be replaced, and as a consequence the physicochemical properties of a clay mineral change. For example,

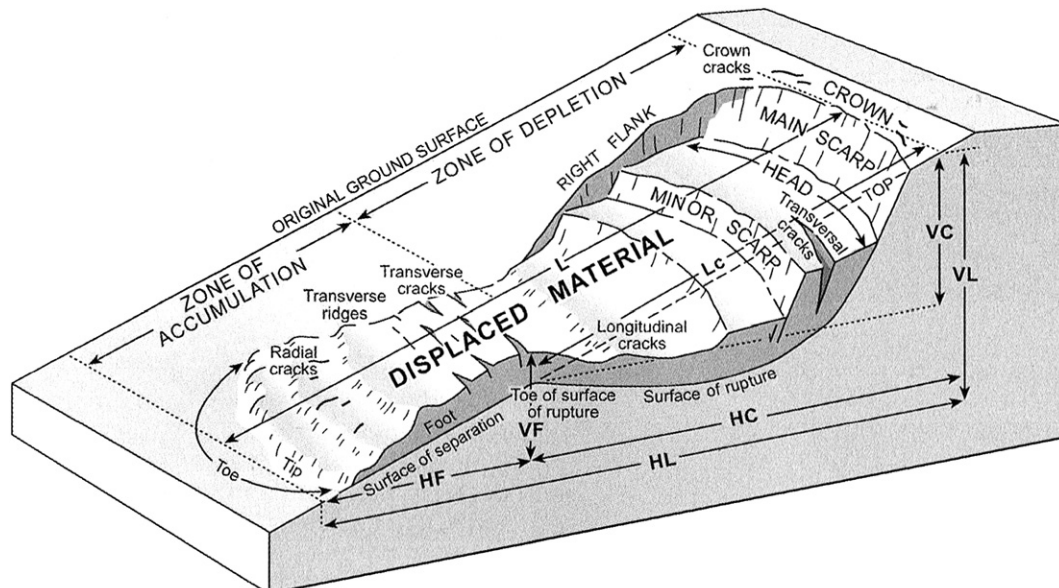
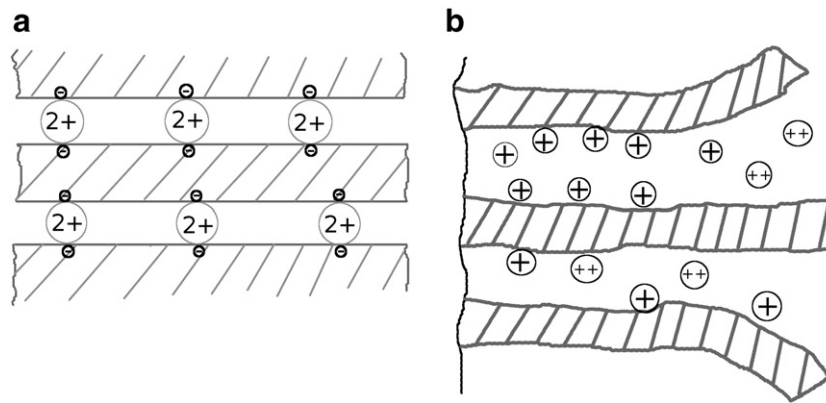


Fig. 1. Scheme of a rotational landslide (Glade et al., 2005, based on Varnes).



**Fig. 2.** Schematic illustration of ionic binding of clay mineral layers: a) Strong ionic binding between clay layers; b) Partial collapse of clay mineral layers by penetration of univalent ions.

$Al_{3+}$  can replace  $Si_{4+}$ , whereby the negative electric charge increases. This action is reversible under positive electric charge conditions. If the electric charge of three-layered clay minerals is weak, a hydration hull surrounds the cations between the ligands. This causes a swelling of the clay minerals. Normally this hull encloses single cations. The hydration hull decreases binding forces between the clay minerals, resulting in an increase of water infiltration into the clay mineral. This process is self-energising and can cause a total collapse of the bonds between the clay minerals (Fig. 2b).

This demonstrates that the pre-condition for ionic replacements is a negative electric charge. This charge can develop by isomorphic replacement of high-ordered cations by low-ordered cations in the crystallized structure, and by dissociation of near-surface  $H$  ions. The negative charge is compensated by an equivalent ratio of positive charge of cations.

Hereby the pattern of adsorption does not only depend on the ions of the soil fluids but also from the ionic charge of these specific ions. If univalent ions occur in a much higher concentration than polyvalent ions, the interchanger favours the univalent ions. This is due to the surplus supply of univalent ions. Univalent ions decrease the strength between clay minerals causing a weakness of clay stability. This reduction in strength might be an important factor for destabilization.

However, this forced reduction in shear strength due to physicochemical conditions is only indirectly incorporated by variations of  $c$  and  $\phi$  in most stability models. The effect of physicochemical influences on these two parameters is not quantified yet. This study wants to demonstrate that this effect might be important for some slope units.

### 3. Research area

The research area of Manaihan is located in the Pays de Herve, a region in eastern Belgium, about 25 km N–E of Liège. This region has a maximum elevation of about 300 m and a local relief of 80–100 m (Fig. 3). The mean slope angle is approximately  $10^\circ$  and ranges between  $0^\circ$  and  $15^\circ$ . The two main rivers, “Berwinne” and “Vesdre” separate the main ridge of the Pays de Herve and drain towards the West (Fig. 3). The geology is characterised by well-preserved Cretaceous formations on Upper Carboniferous rock. The Cretaceous rocks contain silt-like Aachen sands at the base, followed by layers of Vaals clays, and covered by Gulpen chalk. Chalk outcrops are located only at the highest locations of the ridge. The surface is deeply weathered, in some locations up to 4 m. Tectonically the whole area was involved in the Variscian folding. Additionally, the Pays de Herve region is also influenced by the Quaternary lowering of the lower Rhine valley, visible at the Minere trench crossing the region in straight N–S direction.

The landslides in the Pays de Herve are located on the border of this Minere trench, commonly at the contact between the Aachen

sands and the Vaals clay. The landslide prone slopes have an average angle of  $8\text{--}12^\circ$ . Most of these landslides show a complex movement including a rotation in the upper part and a translational slide on the lower part of the landslide (Demoulin et al., 2003). This complex movement is reflected in the landslide topography. First movements have been dated to 1800 BP and it is suggested, that these failures were triggered by an earthquake (Demoulin et al., 2003). The main scarps of these landslides are up to 17 m high and show an inclination of  $45^\circ$  to  $60^\circ$ . Landslides headscarps are located at the base of the Vaals clays. Where the Aachen sands are not covered by the Vaals clays, areas seem to be more stable (Demoulin et al., 2003). After the first phase of landslide activity between 1850 and 1600 BP there were no further incidences of movement (Demoulin et al., 2003). This period is considered as a dormant phase. After 1950 a new phase of activity started. The observed Manaihan landslide was reactivated in the 1970s. In 1966, an industrial sewage pipe crossing this landslide contour-parallel was constructed and put into operation in 1967.

Following heavy rainfall, the most recent movements of some landslide parts started in 1998. Since then these parts have continued to move. Fig. 4 shows considerable infrastructural damage including the cracked sewage pipe. If the pipe has been broken before the movement or broke during the movement is unknown. The general landslide shows a brittle failure. The active landslide parts are characterised by very high water content. After heavy rainfall events, the water table even reaches the surface and ponds appear in the small depressions. On the surrounding dormant landslides such ponds have not been observed on the surface.

The current active landslide is framed by two sewage pipe breaks on the northern (shown on Fig. 4) and southern end. There, the ground collapsed and caused considerable damage, now visible at two excavations at the pipe. Both excavations are covered with plastic sheets to reduce the seepage of rain and protect the infiltration of overland flow into the ground. In order to display the general landslide pattern in 2002, a geomorphological map was compiled (Fig. 5, refer to Demoulin and Glade (2004) for details).

### 4. Methods

The methods applied in this study include surface and subsurface investigations, laboratory analysis of soil and waste water samples and the application of slope stability modelling. Core and cone penetration tests were performed in the field. Two inclinometers were installed on 20/09/2001 at MAN03 and 12/03/2002 at MAN07 (Fig. 5). The borehole MAN03 is located up slope of the sewage pipe, borehole MAN07 down slope (Fig. 6). The inclinometer readings were taken in 0.5 m intervals. Shearing destroyed soon both inclinometers, MAN03 in March 2002 and MAN07 in June 2002.



### Geological setting of the Pays de Herve landslides

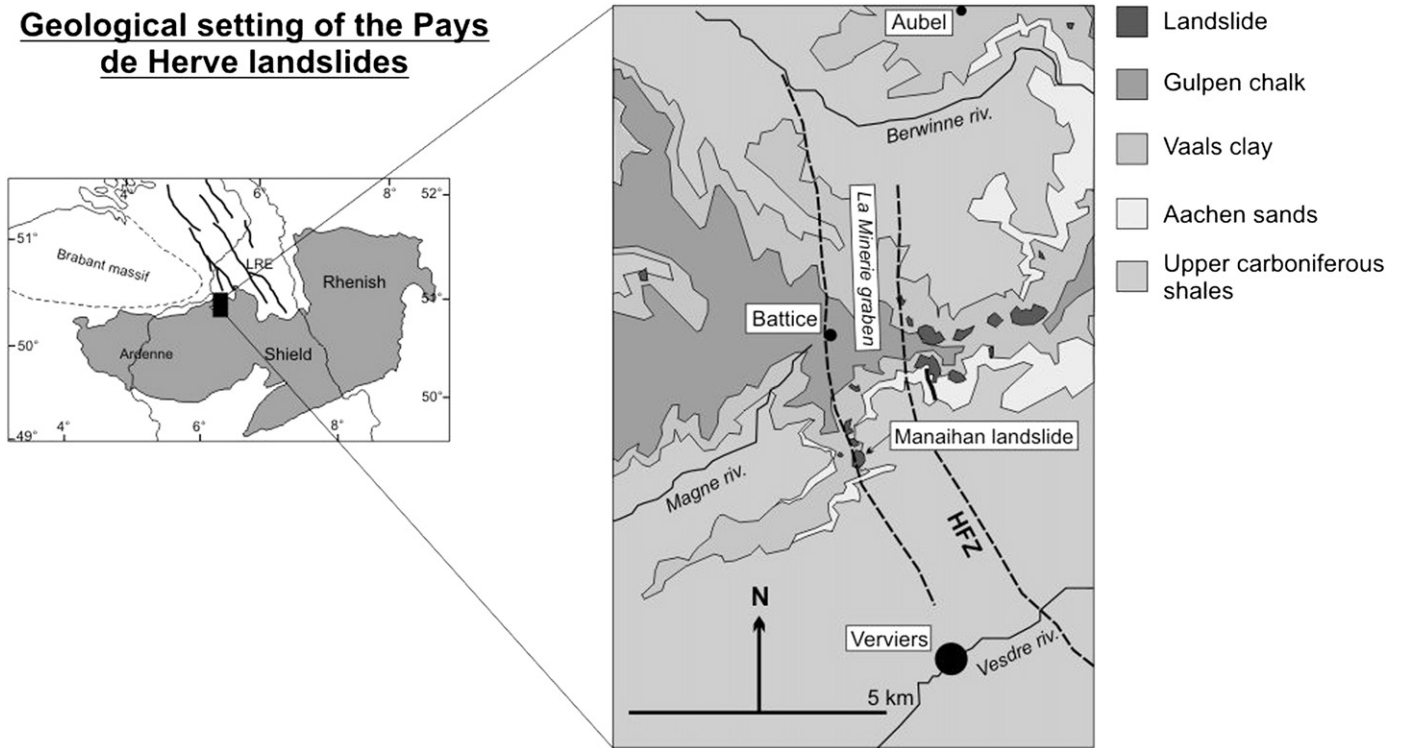


Fig. 3. Geological overview and landslide locations in the Pays de Herve; HFZ: Hockai Fault Zone (Demoulin and Glade, 2004).

For the laboratory analyses 60 soil samples were collected from the cores. The analyses determined several soil properties including grain size distribution,  $\text{CaCO}_3$  content, organic carbon, pH values, and the anion and cation concentrations. Grain size distribution was determined based on Stoke's law (Schachtschabel et al., 2003).  $\text{CaCO}_3$  content was measured with the Scheibler method (Schachtschabel et al., 2003). To calculate the ratio of organic carbon, the samples were heated up to 800 °C. The content of ions in the soil was determined by following the

German Industrial Norm DIN 38414. Additionally 24 waste water samples were collected with a temporal collection interval of 25 h in order to determine the waste water compositions for different days and times within the days. This waste water was analyzed for ionic loading in the laboratory. The slope stability modelling was carried out using the GGU-Stability software, a 2D slope stability tool to calculate the Factor of Safety using geotechnical parameters for respective soil properties. This model is widely used in German geotechnical engineering. The



Fig. 4. The Manaihan landslide area looking upslope with approximate locations of the sewage pipe and the vertical profile of Fig. 6 including locations of the boreholes (Figs. 5, 6, and 9): a) infrastructural damage at the landslide scar, b) exposed sewage pipe (Note: Photograph is turned 90° to illustrate position on landslide).

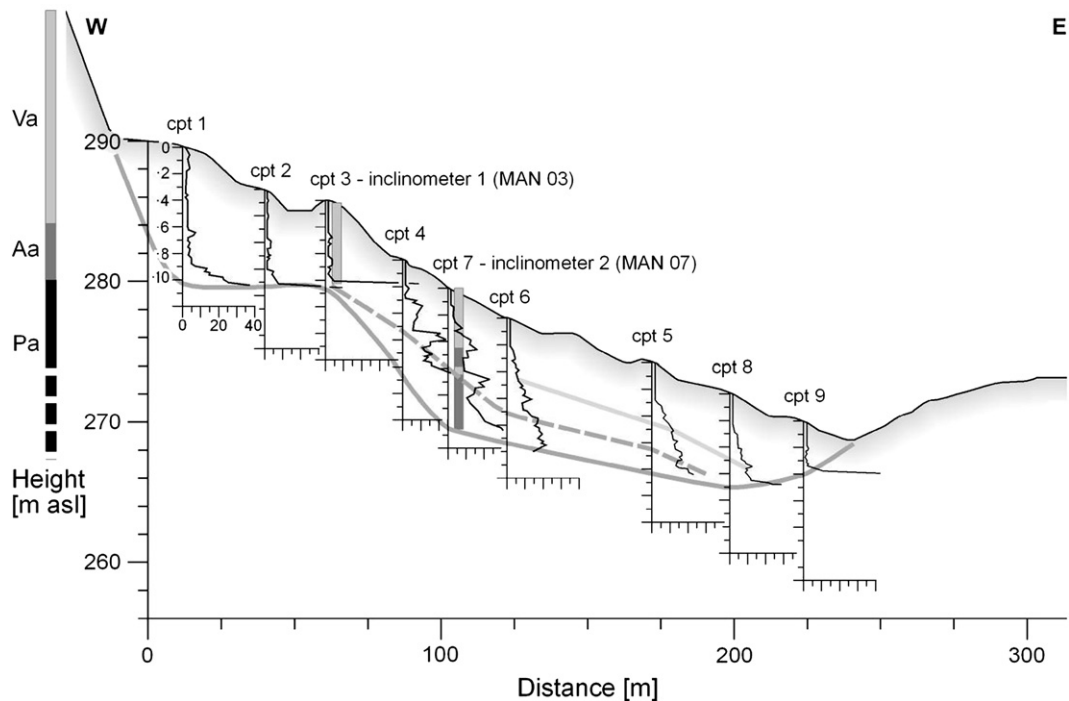


**Fig. 5.** Profile of the landslide with cpt values (Va = Vaals clay, Aa = Aachen sands, Pa = Paleozoic rock). Solid bold grey line represents assumed shear plane of failure body of ancient landslide, dark dashed line represents alternative shear plane of ancient landslide; light solid line represents the shear plane in lower part of the landslide body; vertical bars at MAN03 and MAN07 indicate geological layer composition of the cores.

geometric profile used in this model is based on the cone penetration tests. In addition, the coordinates of GPS-measurements from surface points (Demoulin and Glade, 2004) and the readings of both inclinometers MAN03 and MAN07 have been used to determine the shear plane in this profile. The location of the two boreholes and the two inclinometers MAN03 and MAN07, respectively are also within this geometric profile.

Bishop's (1954, 1960) methods were applied to model slope stability. The pore water conditions were added into the model as groundwater pressures. The physical parameters of the soil have been defined by grain size distribution and significant changes in soil colour and were used to identify different layers. Geotechnical soil properties include the internal

friction angle and cohesion. Two different conditions important for the modelling procedure were assumed:

1. Values for cohesion and internal friction angle are similar in the region for the identical horizons. Thus, respective values were transferred from another site with similar soil characteristics (Table 1, based on Demoulin and Pissart, 2000). Positive pore water pressure was approximated assuming total saturation.
2. The cohesion is zero. Because the landslide is reactivated, the shear strength is negligible (Nash, 1987; Demoulin et al., 2003). The internal friction angle is based on laboratory values assuming fully saturated soil conditions.

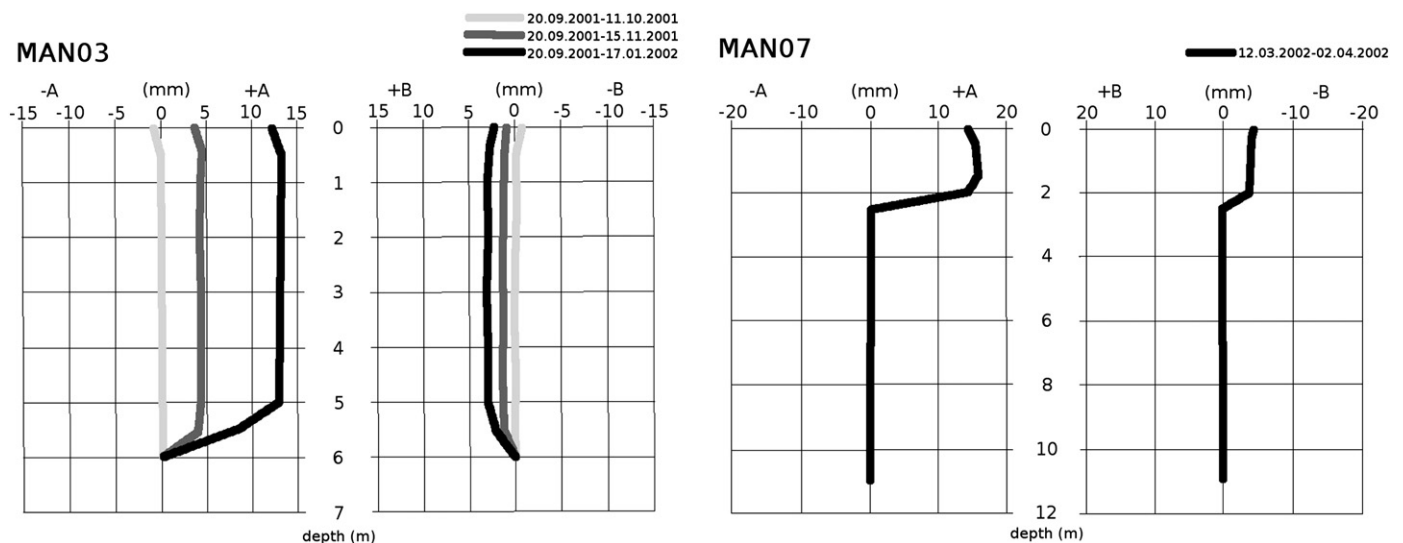


**Fig. 6.** Inclinometer values of the boreholes MAN03 and MAN07; note the different horizontal and vertical scales of a) and b). -A to +A is the downslope direction, -B to +B is perpendicular to the slope, refer to Figs. 4–6 for inclinometer positions on the slope.

**Table 1**

Assumed soil properties provided by Demoulin and Pissart (2000).

Layer	$\rho$ [g/cm <sup>3</sup> ]	$\varphi$ [°]	$c$ [kN/m <sup>2</sup> ]
Soil	2.0	18	31.4
Marl	1.0	15	10.0
Bedrock	2.6	30	50.0

Based on these assumptions four modelling scenarios were calculated: Scenario 1 – the laboratory values for  $\gamma$  and  $c$  were used, scenario 2 –  $\gamma = 0$  and laboratory values for  $c$  were applied, scenario 3 includes lab values for  $\gamma$  and  $c = 0$ , and the worst-case scenario 4 was performed with  $\gamma = 0$  and  $c = 0$  (Table 2). For simplicity  $\rho$  was never changed. It is evident that in some scenarios we assume liquified horizons in the landslide based on observations in the core samples.

## 5. Results

The landslide in Manaihan is a rotational slide with a circular shear plane (Figs. 4–6, refer also to Demoulin and Glade, 2004). This is shown by the significant rise in soil resistance at the lower sections of the cpt points 1–3 for the upper part of the landslide (Fig. 7a). Additionally the transition between little and high resistance at MAN03 is observed at the same depth where the shearing of the inclinometer is located. The foot of the landslide has an approximate location of the shear plane at about 2.50 m depth. The extremely low penetration resistance at cpt 5, 6, 8 and 9 in these first 2.50 m (Fig. 7b) supports this proposed location. The CPT derived resistance values in combination with the data of MAN03 indicate the landslide shear as shown in Fig. 6. The upper CPT profiles cpt1–cpt4 and cpt7 represent the part of slope chosen for stability modelling. Characteristic for this section is soft material until a depth of about 280 m asl, which corresponds to depths of 10 m at cpt1, 7 m at cpt2, 6 m at cpt3, 2 m at cpt 4 and near surface at cpt 7 (Fig. 6). At cpt4 the more resistant material is located at depths of 3.50 m, 5 m–6 m and 8 m. At cpt7, the resistant horizons are at 3.50 m–5 m, 6 m–8 m and from 8.50 m onwards until the end of the core.

The recent movement involves approximately half the area of the ancient landslide. GPS-measurements showed that the new landslide has moved about 40 cm since the start of the monitoring (Demoulin and

Glade, 2004). The inclinometer MAN03 was put into operation on 20/09/2001 and remained active until March 2002 (Fig. 6). Three measurements were taken during this period. Fig. 7 displays clearly the shearing plane at a depth of about 6 m.

Within the first 21 days the landslide moved upslope, which is indeed purely an artefact due to the inclinometer settlement after installation. Within the second interval of 35 days the downslope movement was about 5 mm and showed lateral displacement of 2 mm. This data does not provide information whether the movement is continuous or of discrete intervals. We assume a continuous movement, based on witness reports and visual field observation during 6 months. The last measurement before shearing, 97 days after the first reading, gave a total downslope movement of 13 mm and a lateral displacement of 3 mm. The inclinometer MAN07 (Fig. 7) was installed on 12/03/2002. Only the first reading from April 2nd 2002 was possible. Within that 21-days interval 16 mm downslope movement and 4 mm lateral movement was determined. On 23/04/2002 this inclinometer was destroyed at a depth of 2.50 m. This indicates a horizontal displacement of at least 50 mm which is necessary to crack the inclinometer tube. A distinct shear plane is evident and both inclinometer readings give similar displacement rates from the surface down to the shear plane. This is typical for a block-like movement.

The cores of MAN03 and MAN07 at the sites of cpt3 and cpt7 respectively were also used to take soil samples for determining the grain size distributions. There exist some totally liquefied horizons in the landslide mass. On MAN03 (Fig. 8) more than 90% of the grains contain clay and silt. The content of clay is never below 30% except at a depth of about 6 m. This composition of clay and silt fits to the general composition of Vaals clays. The vertical location is, in relation to the undisturbed elevation of the Vaals clay layer, slightly below. This change in horizon height of similar material strengthens the interpretation of a reactivated landslide. The original elevation of the surface before the first landslide occurred was about 290–295 m asl, which corresponds to the head scarp of the Manaihan landslide.

The grain size distribution of borehole MAN07 (Fig. 8) is not that distinct. The first 2.50 m from the surface are dominated by clay, with a proportion of almost 60%. From 3 m to 8 m depth the silt fraction is most dominant. The depth from about 7.50 m to 8.50 m is characterized by high sand fraction, up to 70% at 7.80 m. Further down, the clay and silt fraction has the highest proportion. The sand fraction ratio is up to approximately 70% at a depth of 7.50 m. Related to the undisturbed layers, this grain size distribution displays a strong vertical mixing of the Vaals clays and the Aachen sands (Fig. 6).

The chemical characteristics are described for MAN03 and MAN07 in Figs. 8 and 9. The pH-value on MAN03 is generally higher than 5. There are two changes in a depth of about 2 m with a value increase from pH 5 to pH 6.5 and one in the depth of 3.50 m increasing from pH 6.3 to pH 7.3. These high values remain until the maximum depth. There are also some peaks in the concentrations of the ions. Again the values increase at a depth of 2 m and at 3.50 m. But in contrast to the pH values the ion content decreases again at 4.80 m and remain relatively constant until 5.80 m. The ion content rises again further down to those reached previously between 3.80 and 4.80 m. The curve of  $SO_4$  shows differences in its pattern compared to the other concentrations of anions. Below the depth of 3.50 m the concentration increases up to more than 1000 mg/kg soil until a depth of 4.60 m. Further down the concentration reduces again to less than 100 mg/kg. At about 5.80 m there is a secondary peak of concentration, again exceeding 1000 mg/kg.

MAN07 is characterized by different concentrations. The pH-value is between 5 and 6 up to the depth of almost 2 m, followed by a sequence of pH-values between 7 and 8.3. This sequence continues to a depth of 5.50 m. In deeper areas the pH decreases below 6. At 7.70 m the pH value is 4.1. At a depth of 8.90 m the value increases to 5 and remains stable until 11 m. The upper 4 m of the core show intense variations in the concentration of ions in the soil. From a depth of 5–6 m to the bottom of the core the distribution is more uniform. The concentration

**Table 2**Different modelled scenarios including applied geotechnical parameters  $\varphi$ ,  $c$  and  $\gamma$  and the Factor of Safety  $F$ .

Layer	$\varphi$ [°]	$c$ [kN/m <sup>2</sup> ]	$\gamma$ [N/m <sup>3</sup> ]	$F$
Scenario 1				
Soil	18	31.4	19.62	3.03
Marl1	15	10.0	9.81	
Marl2	15	10.0	9.81	
Marl3	15	10.0	9.81	
Bedrock	30	50.0	25.51	
Scenario 2				
Soil	0	31.4	19.62	2.33
Marl1	0	10.0	9.81	
Marl2	0	10.0	9.81	
Marl3	0	10.0	9.81	
Bedrock	0	50.0	25.51	
Scenario 3				
Soil	18	0	19.62	0.75
Marl1	15	0	9.81	
Marl2	15	0	9.81	
Marl3	15	0	9.81	
Bedrock	30	0	25.51	
Scenario 4				
Soil	0	0	19.62	0.00006
Marl1	0	0	9.81	
Marl2	0	0	9.81	
Marl3	0	0	9.81	
Bedrock	0	0	25.51	

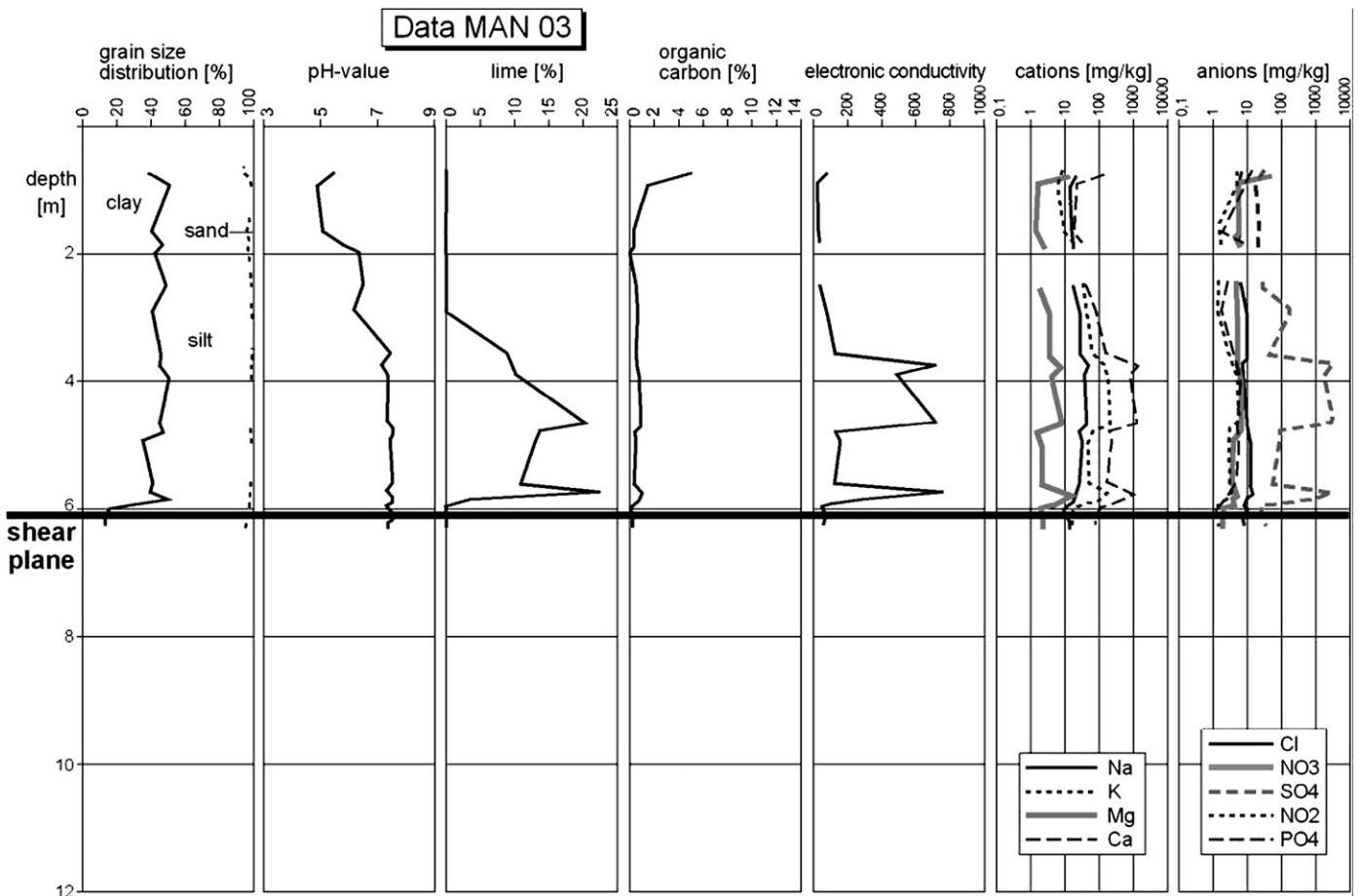


Fig. 7. Grain-size distribution and geochemical properties for core MAN03.

of  $Ca$  and  $SO_4$  increases to an ionic content 100 times larger than the other values. It remains at this level until the final depth of 11 m. Here only the ions of  $Ca$  and  $SO_4$  rise. This is in contrast to MAN03, where the concentrations of  $Ca$ ,  $Mg$ ,  $K$  and  $SO_4$  change synchronously. In both cores, the concentrations of  $Na$  and  $Cl$  remain stable within the total depth and thus show a different pattern than the other ions.

The applied geotechnical data determining the initial characteristics of the soil were taken from Demoulin and Pissart (2000). These data were averaged from laboratory measurements on samples representative of the Aachen and Vaals formations in the study area (Table 1). Due to the different grain size distribution, the marl layer is divided into three sections for slope stability modelling. In total four scenarios were modelled (Table 2). Within the first and second scenario a Factor of Safety  $F=3.03$  and  $F=2.33$  respectively was calculated. The third scenario gives  $F=0.76$  and the fourth scenario ( $\varphi$  and  $c$  were set as 0) result in  $F=0.00006$ . Although the assumptions for the fourth scenario may seem to be implausible, it has to be noted that sections in the core were fully liquified (and by definition have extremely low shear strength). Despite its unlikely appearance, this scenario was also used. Consequently, the stability of this slope is modelled as definitely unstable when both cohesion and internal friction angle are equal to 0. This scenario describes a reactivated landslide with completely saturated conditions (Nash, 1987) which fits to our field and laboratory observations. In any case, the real stability conditions differ definitely from the calculated values due to uncertainties inherent in any modelling approach (Lang et al., 2003).

The results of the waste water analysis give a high mean ionic loading over the sampled time interval (Table 3). These results are not surprising considering the industrial sewage water. Of particular

significance herein is the relatively high value of  $Na$ , which can also be determined in the soil samples.

## 6. Discussion

The focus of the geochemical analysis is on the univalent ions. Only they are able to reduce the cohesion of clays significantly. Those univalent ions are concentrated in different depths in MAN03 and MAN07.  $Na$  and  $K$  are present in relatively high concentrations in both soil and waste water samples. If ionic adsorption of the clays depends on the number of available bindings and on the concentration of ions, the available binding sites will be occupied by univalent ions. In MAN03 the peaks of ionic concentration is within 4–5 m and at 5 m below surface. These peaks in ionic content do not correspond to a significant change in grain composition ( $R^2=0.4$ ). This may show an independency between grain size distribution and ionic loading of soils, which is contrast to what one might expect. At least in MAN07 there is a weak correlation ( $R^2=0.53$ ) between ionic loading and grain size distribution. But the depth of the highest ionic concentrations in MAN03 may refer to the depth position of the sewage pipe. This may indicate that the loaded water may disperse almost horizontally in both slope directions. This condition can only be met with negligible interflow in the top part of the landslides. Another secondary peak of ionic loading of the soil in MAN03 is near the shear plane. This may indicate favourable conditions for ionic enrichment near this shear plane, probably due to structural damage of the soil particles.

In MAN07 the enrichment of ions is well below both the surface and the shear plane at a depth from 5 m to the bottom of the core. This may indicate a completely different flow path of the ionic loaded water in



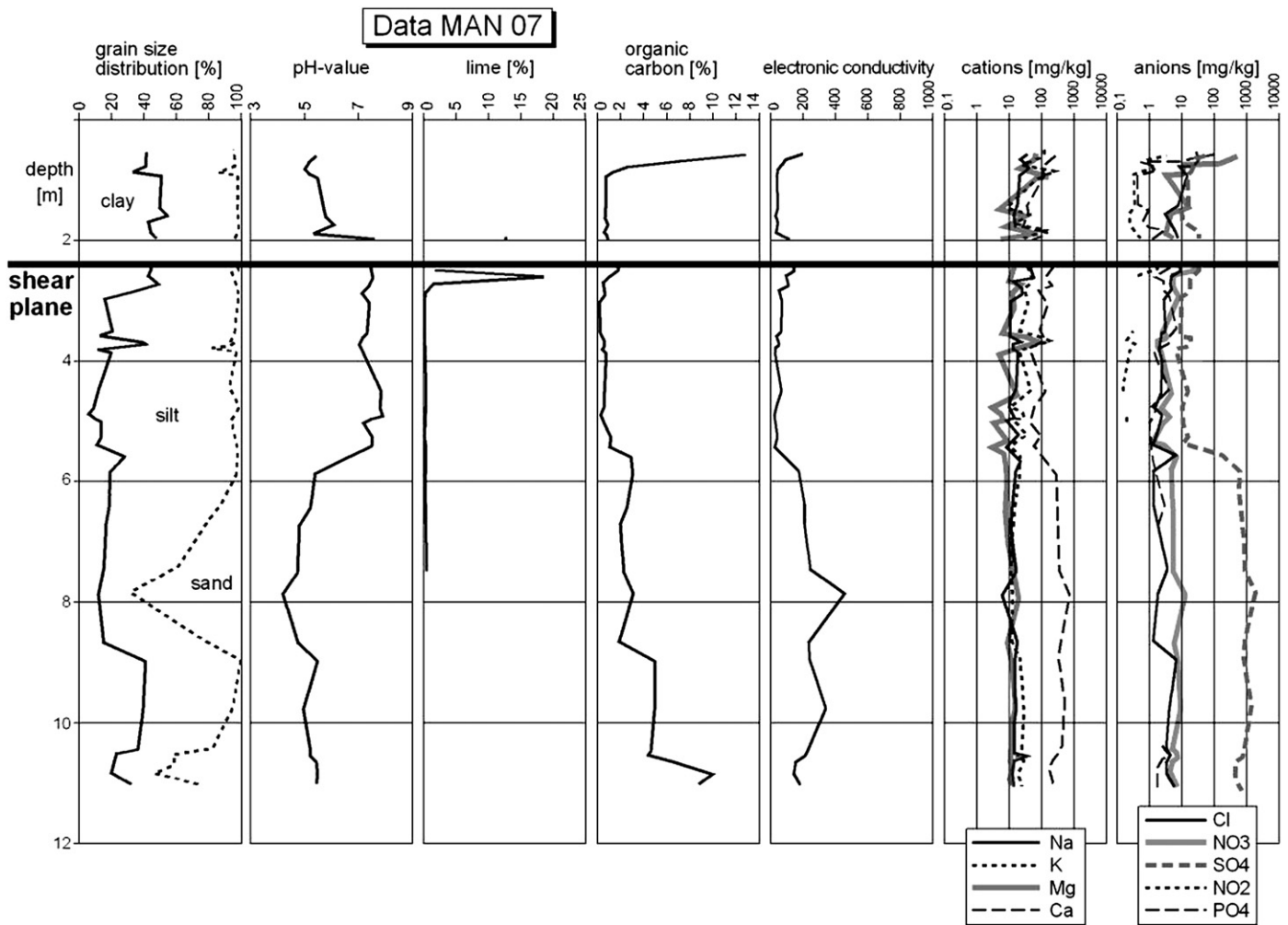


Fig. 8. Grain-size distribution and geochemical properties for core MAN07.

the slope. Possibly, the water flows from the sewage pipe along a zone of weakness, which is in contrast to MAN03. In MAN07 the water does not distribute horizontally or along the shear plane but in a horizon which is more dominated by the Aachen Sand formation (Fig. 6).

The general amount of ions attached to the soil particles should be higher in MAN07 than in MAN03 due to its down slope location. This expected distribution cannot be verified by the mean concentrations of ions in the soil samples of MAN03 and MAN07 (Table 3). The overall concentration of ions is higher in MAN03 than in MAN07. This may indicate that above the sewage pipe there exists another soil water regime. It can be assumed that above the pipe the soil water percolation is highly reduced and thus favours higher concentrations of ions in the soil. In contrast the area below is characterized by an increased water percolation through the slope preventing the ions from remaining in the soil and removing them by constant drainage. This interpretation may be confirmed by the high water content of the soil samples in MAN07. As described above, the soil in the core was sometimes totally fluidized.

The laboratory analysis of the soil samples and the waste water give high  $\text{Na}^+$ , which is able to destabilize soils (Veder and Hilbert, 1981).  $\text{Na}$  is not bound in soils for long periods, and is thus removed quickly. However, its high concentration in the soil samples may cause a saturation of the ionic exchangers, even for a short time. Czurda and Xiang (1993) found that the allocation of cations influences the slope stability. Clays with  $\text{Ca}$  and  $\text{K}$  as ions are dispersed, other ions cause a flocculated clay structure. This indicates a reduced absorbing capacity for  $\text{Ca}$  and  $\text{K}$  in a dispersed structure. According to Czurda and Xiang

(1993) the shear parameters with lowest values are found in marls containing  $\text{Na}^+$ . This  $\text{Na}^+$  was also the most highly concentrated univalent ion found in the water samples.

The varying modelling assumptions give different results. Modelling results determine slope instability only if the cohesion and the internal friction angle are equal to 0 (=scenario 4). This can only be expected under completely saturated conditions for a reactivated landslide. The scenario 3 with  $F=0.76$  results also in instability. If uncertainty margins would be additionally added to both Factor of Safety calculations (Lang et al., 2003) slope conditions can be regarded as highly unstable. In reality, this calculated instability refers to an actually stable slope. Thus this Manaihan landslide still has some retaining shear strength, however, slope stability must be in a highly critical state, obviously near failure.

The first hypothesis, that the human factor influences landslide behaviour, is similar to a case described by Hancox (2002). He describes a landslide, which occurred in 1979 in Abbotsford, New Zealand, as being strongly influenced by human factors. The region affected by the landslide was lithologically dominated by clayey loess and gravel overlying Tertiary sediments. At that location, a sand quarry at the foot of the slope and high groundwater levels were proposed as the main factors in destabilizing the slope and leading to landslide occurrence. The high groundwater levels were attributed to a leaking aqueduct above the landslide area. Parallels between the Abbotsford landslide and the Manaihan landslide are the existence of water supply in form of leaking water and the cut into the slope. Although different in location (in Abbotsford at the toe, in Manaihan in the middle section of the



**Table 3**

Mean values of ionic loading of waste water between 06/02/2003 and 03/03/2003 and from the soil samples of MAN03 and MAN07.

Type of ions	In waste water [mg/l]	In MAN03 [mg/kg]	In MAN07 [mg/kg]
<b>Cations</b>			
Na	45.443	23.49	19.23
K	8.804	64.94	43.70
Mg	4.394	4.64	22.45
Ca	98.651	310.68	173.41
<b>Anions</b>			
Cl	81.515	9.66	5.28
NO <sub>2</sub>	–	1.67	0.32
NO <sub>3</sub>	19.208	7.60	21.70
PO <sub>4</sub>	0.209	2.81	4.93
SO <sub>4</sub>	78.154	690.98	186.13

landslide), the major issue herein is that the natural landslide geometry was disturbed and totally different forces have been – unintentionally – employed.

In Manaihan the perpendicular cut during the installation of the pipe might have enhanced slope sensitivity to internal and external factors. These changes might have led to a reduced threshold for landslide initiation, which was exceeded in the 1990s. This heavy rainfall event triggered the landslide. Once initiated, this motion continued. It can be assumed that the moving mass bent the pipe and partially destroyed it. Ion rich waste water from the pipe leaked into the slope and percolated through the deeper parts of the landslide mass, leading to an almost completely saturated soil, even in drier periods. Consequently, the ion concentration in the soil might have increased. These ions were able to destabilize the clays in the soil and favoured water circulation between the clay layers. This might have resulted in continuously reduced slope stability, with the result that the Manaihan landslide remains active even during rainfall events of very low magnitude. There is some field evidence (e.g. constantly saturated conditions in the foot of the landslide) that this slope is always in a state near the threshold for movement. This condition is maintained by continued leakage from the sewage pipe and thus, even minor rainfall events might reactivate this landslide.

This interpretation cannot be proven empirically in this study, but it can be expected that the sewage pipe loses sufficient ion-loaded water to influence slope movement significantly. From the foregoing observations and analysis, there is a clear indication that the high content of water in the slope, the high concentration of univalent ions in the soil, the partial source of the soil water from the industrial waste water and the continuous movement might be factors which lead to a permanently unstable slope condition.

## 7. Conclusions

The building of the sewage pipe is an anthropogenic impact with a long-lasting influence, in particular for the investigated slope. It is proposed that this installation disposed the slope and a rainfall event in 1998 initiated the first reactivation. Many other similar old and dormant landslides exist in the same geological and morphological situation, but these were not reactivated during that particular rainfall event. We assume the installation of the sewage pipe preconditioned the slope for failure. The initial movement of the slope caused the successive damage to the sewage pipe. This damage resulted in an increase of water leakage. The leaking water was loaded with various ions, including many univalent ions. The discharge of waste water and the ions promoted the movement by reducing the shear strength of the soil. In addition, the leaking water resulted in saturated slope conditions. This saturation reduced the friction angle and may even partially liquefy some soil horizons or layers in the slope. But, as the modelling results show, a complete saturation is not sufficient to initiate slope movement. Cohesion is the crucial value we assumed to

be 0, but other investigations have shown, that this, even in reactivated landslides, is not always the case (Kenney, 1984).

The ionic concentration may emerge as an important factor in stability assumptions, because it can reduce the cohesion of the soil material. As mentioned the extent of the reduction of cohesion is not determined quantitatively in this study. To do so, more emphasis has to be taken on the soil in undisturbed conditions in order to compare it to our soil samples from disturbed locations and on the monitoring of relevant parameters.

The results of the landslide stability analysis indicate, that the slope may fail if certain assumptions of geotechnical soil properties are made. Comparing these research results with conclusions from slope stability analysis of clay-rich soils (Kenney, 1984; Czurda and Xiang, 1993), Gudehus and Külzer (2002) shows that such assumptions are not possible in slopes. Consequently, cohesion and internal friction angle generally cannot both be equal to 0, as we calculated them assuming the above stated conditions. Nevertheless, the core samples of MAN03 and MAN07 showed sections of fluid soil. Gudehus and Külzer (2002) explicitly mention that conventional methods of soil mechanics are not sufficient for an appropriate investigation with respect to geochemical loadings of the soil.

The slope stability modelling based on geochemical properties is not yet a common analytic technique. It is demonstrated, however, that in clay-rich soils factors other than just mechanical ones may also play important roles in slope stability. The complexity of the chemical influence is much greater than those presented here and thus still difficult to assess. To verify the results it is necessary to investigate the field site in the future in more detail to compare soils which are not affected by the landslide with our soil samples, to trace the groundwater and wastewater flow paths and to quantify the concentration of univalent ions required for failure for previously presented conditions.

Field measurements, laboratory experiments and modelling procedures are necessary to understand and explain the movement pattern of the Manaihan landslide. Such procedures are indispensable for an improved understanding of the slope and for the determination whether a chemical influence exists on total slope stability, or if this chemical influence is negligible for slope stability analysis. This question and the resulting answers are critical for understanding landslide movement where complex physical and geochemical factors are involved.

## Acknowledgements

The Authors thank Mr. and Mrs. Leruth for permission to use their land for field testing. The staff of the geotechnical laboratory at University of Bonn receives our sincere thanks for performing the analysis. We finally want to deeply acknowledge the reviewers Michael Crozier and Jack McConchie for their critical comments leading to an improved manuscript.

## References

- Anderson, M.G., Richards, K.S., 1987. Modelling slope stability: the complementary nature of geotechnical and geomorphological approaches. In: Anderson, M.G., Richards, K.S. (Eds.), *Slope stability*. Wiley, Chichester, pp. 1–9.
- Barnard, P.L., Owen, L.A., Sharma, M.C., Finkel, R.C., 2001. Natural and human-induced landsliding in the Garhwal Himalaya of northern India. *Geomorphology* 40, 21–35.
- Bishop, A.W., 1954. The use of the slip circle in the analysis of slopes. *Geotechnique* 5, 7–17.
- Bishop, A.W., 1960. Stability coefficients of earth slopes. *Geotechnique* 10, 129–150.
- Craig, R.F., 1992. *Soil mechanics*. Chapman and Hall, London.
- Crozier, M.J., 1989. *Landslides – causes, consequences and environment*. Routledge, London.
- Cruden, D.M., Varnes, D.J., 1996. Landslide types and processes. In: Turner, A.K., Schuster, R.L. (Eds.), *Landslides: investigation and mitigation*. Special Report. National Academy Press, Washington, D.C., pp. 36–75.
- Czurda, K., Xiang, W., 1993. Der Einfluss der Kationenbelegung auf das Kriechverhalten von Tonen am Beispiel einer ostalpinen Grosshangbewegung. Proceedings of the 9. Nationale Tagung für Ingenieurgeologie, Garmisch-Partenkirchen, pp. 33–42.

- Demoulin, A., Glade, T., 2004. Recent landslide activity in Manaihan, East Belgium. *Landslides* 4, 305–310.
- Demoulin, A., Pissart, A., 2000. *Les glissements de terrain du Pays de Herve*. Unpublished Report of the Walloon Region Convention 99/42075.
- Demoulin, A., Pissart, A., Schröder, C., 2003. On the origin of late Quaternary palaeolandslides in the Liège (E-Belgium) area. *International Journal of Earth Sciences* 92, 795–805.
- Gillon, M.D., Denton, B.N., Macfarlane, D.F., 1991. Field investigation of the Cromwell Gorge landslides. In: Bell, D. (Ed.), *Landslides*. Balkema, Rotterdam, pp. 111–118.
- Glade, T., 2003. Landslide occurrence as a response to land use change: a review of evidence from New Zealand. *Catena* 51, 297–314.
- Glade, T., Anderson, M.G., Crozier, M.J. (Eds.), 2005. *Landslide hazard and risk*. Wiley, Chichester.
- Goudie, A., 2006. *The human impact on the natural environment*. Blackwell Publishing, Oxford.
- Gudehus, G., Külzer, M., 2002. Einfluss von Ionen und Gasblasen auf die Kollapsneigung feinstkörniger Böden. *Geotechnik* 25, 12–19.
- Hancox, G.T., 2002. The Abbotsford landslide — its nature and causes. *Tephra* 19, 9–13.
- Hartge, K.H., Horn, R., 1991. *Einführung in die Bodenphysik*. Spektrum Akademischer Verlag, Stuttgart.
- Hendron, J.A.J., Patton, F.D., 1987. The Vaiont slide — a geotechnical analysis based on new geologic observations of the failure surface. *Engineering Geology* 24, 475–491.
- Kenney, C., 1984. Properties and behaviours of soils relevant to slope instability. In: Brunsden, D., Prior, D.B. (Eds.), *Slope Instability*. Wiley, Chichester, pp. 27–65.
- Kronberg, B.I., Nesbitt, H.W., 1981. Quantification of weathering, soil chemistry and soil fertility. *Journal of Soil Science* 32, 453–459.
- Lang, H.-J., Huder, J., Amann, P., 2003. *Bodenmechanik und Grundbau*. Springer, Berlin.
- Nash, D., 1987. A comparative review of limit equilibrium methods of stability analysis. In: Anderson, M.G., Richards, K.S. (Eds.), *Slope Stability*. Wiley, Chichester, pp. 11–75.
- Petley, D.N., Higuchi, T., Petley, D.J., Bulmer, M.H., Carey, J., 2005. Development of progressive landslide failure in cohesive materials. *Geology* 33, 201–204.
- Remondo, J., Soto, J.S., Gonzalez-Diez, A., de Teran, J.R.D., Cendrero, A., 2005. Human impact on geomorphic processes and hazards in mountain areas in northern Spain. *Geomorphology* 66, 69–84.
- Runqiu, H., Lungsang, C., 2003. Human-induced landslides in China: mechanism study and its implication on slope management. *Chinese Journal of Rock Mechanics and Engineering* 23, 2766–2777.
- Schachtschabel, P., Blume, H.P., Brümmer, G., Hartge, K.H., Schwertmann, U., 2003. *Lehrbuch der Bodenkunde*. Enke, Stuttgart.
- Veder, C., Hilbert, F., 1981. *Landslides and their stabilization*. Springer, New York.
- Zaruba, Q., Mencl, V., 1969. *Landslides and their control*. Elsevier, Amsterdam.